

- N. Y., McGraw-Hill, pp 187-196.
- Hartzell, C. R., Bradshaw, R. A., Hapner, K., and Gurd, F. R. N. (1968), *J. Biol. Chem.* 243, 690.
- Janssen, L. H. M., DeBruin, S. H., and Van Os, G. A. J. (1970), *Biochim. Biophys. Acta* 221, 214.
- Janssen, L. H. M., DeBruin, S. H., and Van Os, G. A. J. (1972), *J. Biol. Chem.* 247, 1743.
- Katz, S. (1972), *Methods Enzymol. Part C* 26, 395.
- Katz, S., Crissman, J. K., Jr., and Beall, J. A. (1973a), *J. Biol. Chem.* 248, 4840.
- Katz, S., and Ferris, T. G. (1966), *Biochemistry* 5, 3246.
- Katz, S., and Miller, J. E. (1971a), *Biochemistry* 10, 3569.
- Katz, S., and Miller, J. E. (1971b), *J. Phys. Chem.* 75, 1120.
- Katz, S., and Miller, J. E. (1972), *J. Phys. Chem.* 76, 2778.
- Katz, S., Miller, J. E., and Beall, J. A. (1973b), *Biochemistry* 12, 710.
- Kauzmann, W., Bodanszky, A., and Rasper, J. (1962), *J. Amer. Chem. Soc.* 84, 1777.
- Krausz, L. M. (1970), *J. Amer. Chem. Soc.* 92, 3168.
- Linderström-Lang, K., and Lanz, H. (1938), *C. R. Trav. Lab. Carlsberg* 21, 315.
- Peacock, A. C., Bunting, S. L., and Queen, K. G. (1965), *Science* 147, 1451.
- Rasper, J., and Kauzmann, W. (1962), *J. Amer. Chem. Soc.* 84, 1771.
- Sharonova, N. A., Sharonova, Y. A., and Volkenstein, M. V. (1972), *Biochim. Biophys. Acta* 271, 65.
- Steinhardt, J., and Zaiser, E. M. (1953), *J. Amer. Chem. Soc.* 75, 1599.

## Variability in the Tertiary Structure of $\alpha$ -Chymotrypsin at 2.8-Å Resolution†

Alexander Tulinsky,\* Richard L. Vandlen,‡ Carl N. Morimoto,§  
N. Venkit Mani,¶ and Lynn H. Wright||

**ABSTRACT:** The structures of the independent monomeric units of dimeric native  $\alpha$ -chymotrypsin have been compared at 2.8-Å resolution *via* a difference electron density map between the two molecules. Approximately 16% of the density (one-sixth of a molecule) showed differences  $>0.7 \text{ e}\text{\AA}^{-3}$  or three times the expected standard deviation of the difference density. Representative differences in the electron density have been related to variability in the tertiary structure in the two molecules. The variability also manifests itself in a number of other ways: in heavy atom derivatives, in the behavior of localized sulfate ions in crystallographic sulfate-selenate exchange experiments, and in derivatives of  $\alpha$ -chymotrypsin (inhibitors, substrate-like molecules, transition state analogs, changes in structure with change in pH). The largest number of differences resides in the dimer interface region and in a 5-6-Å shell around the surface of the dimer; the smallest number occurs in the interior of the monomeric molecules. The differences in structure are most often associated with the orientation and configuration of side chains and less so with

the main chains. The surface variability probably reflects the relatively large degree of adaptability in tertiary structure in this region of the enzyme and might be a fairly general phenomenon also common to functioning molecules in solution and in biological systems. From the nature of the variability in structure in the dimer interface, the formation of dimer must be accompanied by structurally asymmetrical and dynamical changes in this region of the enzyme. This could conceivably be a characteristic of most oligomeric structures. Aromatic residues tend to aggregate within the molecular structure suggesting a source of stabilizing interactions involving the delocalized electrons of the aromatic side chains. Two sulfate ions participate in a hydrogen bonding scheme which appears to be an important interaction in maintaining the dimeric structure. The ions form bridges, in a reciprocating manner between the independent molecules, which involve the catalytically crucial Ser-195 of one molecule and the phenolic hydroxyl group of terminal Tyr-146 of the other molecule.

At about pH 4.0,  $\alpha$ -chymotrypsin crystallizes from approximately half-saturated ammonium sulfate solutions and the crystals are usually stored at a similar pH but at higher

concentrations of ammonium sulfate (65-75% saturated) (Sigler *et al.*, 1966; Tulinsky *et al.*, 1973). The crystals belong to the monoclinic crystal system, space group  $P2_1$ , with four molecules (mol wt  $\sim 25,300$ ) per unit cell or two molecules of enzyme per asymmetric unit. Consequently, to describe the space arrangement in the crystal precisely and completely, the molecular structures of both crystallographically independent molecules in the asymmetric unit (mol wt  $\sim 51,000$ ) must be determined. The two molecules have been shown to be related to each other by an approximate noncrystallographic twofold rotation axis (local twofold axis) in a manner that interfaces the independent molecules with one another to yield a dimeric unit (Blow *et al.*, 1964; Sigler *et al.*, 1968; Cohen *et al.*, 1970; Tulinsky *et al.*, 1973). Such an interaction is con-

† From the Departments of Chemistry and Biochemistry, Michigan State University, East Lansing, Michigan 48824. Received April 2, 1973. This work was supported by the National Science Foundation, Molecular Biology Section, Grants GB-6586, GB-7399, and GB-15402.

‡ Present address: Chemistry Division, California Institute of Technology, Pasadena, Calif. 91109.

§ Present address: Department of Biochemistry and Biophysics, Texas A&M University, College Station, Tex. 77843.

¶ Deceased, Sept 19, 1972.

|| Present address: Frederick Cancer Research Center, Frederick, Md. 21701.

TABLE I: Heavy Atom Derivatives,  $\alpha$ -Chymotrypsin.<sup>a</sup>

Pt(+)			Pt			Hg			UO <sub>2</sub> <sup>2+</sup>			UO <sub>2</sub> <sup>2+</sup> (+)			U + Au		
Posi- tion	Z	$\delta_2$	Posi- tion	Z	$\delta_2$	Posi- tion	Z	$\delta_2$	Posi- tion	Z	$\delta_2$	Posi- tion	Z	$\delta_2$	Posi- tion	Z	$\delta_2$
1	64	1.10	1	22	0.18	1	63	0.35	U	67	2.10	U	83	2.51	U	95	2.44
1'	68		1'	27		1'	58		U'	17		U'	42		U'	33	
2	48	0.59	2	50	0.73	2	35	0.32	D	10	1.08	D	16	1.62	2	18	0.82
2'	47		2'	44		2'	37		D'	7		D'	14		2'	15	
3	68	0.50	3	66	0.69	A	22	0.21	U-A	14	*	3	17	0.65	3	21	0.80
3'	63		3'	50		A'	20		C	13	*	3'	15		3'	21	
I-2	24	0.74	I-2	25	0.64	B	18	*				F	12	0.52	4	43	*
I-2'	19		I-2'	30								F'	16		C	23	*
4	36	*	4	11	*							C	11	*	E	19	*
U	33	*	U	0											U-A	14	*
I-2a	29	*	I-2a	27	*										a	11	*
I-1	25	*	I-1	10	*										b	12	*
I-1'	18	*	I-1'	11	*										c	12	*
			3a	17	*												

<sup>a</sup> Z, occupancy in electrons;  $\delta_2$ , difference in positions (ångströms) after twofold symmetry operation on one position; an asterisk denotes no twofold counterpart observed.

sistent with the observation that  $\alpha$ -chymotrypsin dimerizes in solution at lower pH values with concomitant decrease in catalytic activity (Steiner, 1954; Egan *et al.*, 1957; Aune and Timasheff, 1971). At higher pH values, the enzyme is monomeric and displays optimal catalytic activity in the vicinity of pH 7.5–8.0. Figure 1 shows a schematic representation of the dimeric structure in terms of the approximate overall shape of the individual monomeric units viewed along the local twofold axis. The position of the local twofold axis can be seen in Figure 1 with respect to the active-site regions (designated by asterisks and located about midway between the surface regions along the local twofold). The arrows in Figure 1 designate the reciprocal manner in which the carboxyl termini of the B chains (Tyr-146) penetrate into the active-site regions of opposing molecules.

An X-ray crystallographic structure determination of tosyl- $\alpha$ -chymotrypsin at 2.0-Å resolution has been carried out by David M. Blow and his collaborators at the Medical Research Council (MRC) in Cambridge, England. The MRC group found that the electron density corresponding to the independent molecules generally contained few significant differences so that the electron density distributions of the individual molecules were averaged about the local twofold axis and the average map was used to obtain a model for the average structure of the two monomers (Birktoft *et al.*, 1969; Birktoft and Blow, 1972). However, the MRC group also recognized that some differences in conformation exist between the two molecules at the last four residues of the A

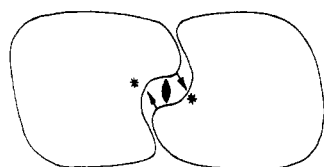


FIGURE 1: Schematic drawing of the dimeric structure of  $\alpha$ -chymotrypsin. Monomeric units related by local twofold rotation symmetry element shown.

chain (10–13), residues 74–77 in the B chain, and in some of the solvent-accessible side chains. The model was built to fit the predominant density and when the average map was ambiguous, the electron density of the individual molecules was examined and the clearer alternative was chosen for the model (Birktoft and Blow, 1972). Finally, with the aid of difference electron density methods, the MRC group was able to relate the tosyl- $\alpha$ -chymotrypsin structure approximately to that of the native enzyme at 2.0-Å resolution (Sigler *et al.*, 1968; Steitz *et al.*, 1969).

Such was not the case with us where significant structural and behavioral differences between the two molecules manifested themselves early in our work and persisted throughout in nearly all phases. Whereas the MRC study involved interchange of parent in the heavy-atom isomorphous derivatives and difference electron density methods to obtain the native structure, our work was more straightforward and was based exclusively on the native enzyme structure, involved a larger number of heavy atom isomorphous derivatives, and centered about innovative diffractometric intensity data collecting methods (Vandlen and Tulinsky, 1971a; Tulinsky *et al.*, 1973). This probably made it possible to analyze in more detail the structures of each of the monomers with respect to variability in structure and to investigate indirectly the general chemical behavior of the independent molecules of the asymmetric unit through changes in the structure caused by reaction or interaction with a large number of different irreversible and competitive inhibitors, substrate-like molecules, and transition-state analog complexes. We outline here some results, consequences, and implications of these various observations and comparisons since they bear certain features of general interest, utility, and applicability.

#### Heavy Atom Derivatives

We have been investigating the structure of  $\alpha$ -chymotrypsin since the spring of 1962. Our first indications suggesting possible structural differences between the two molecules came at the time when crystals were still being surveyed for

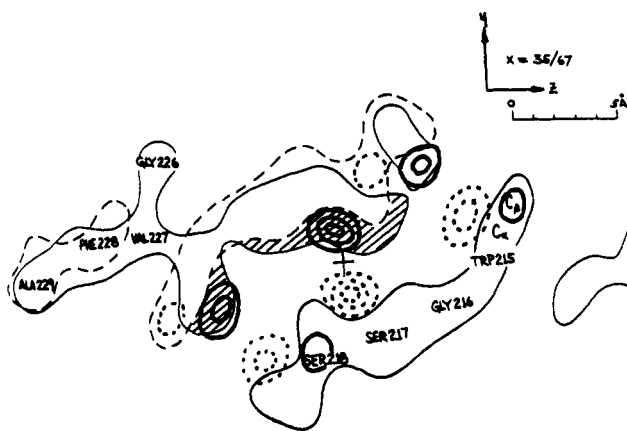


FIGURE 2: Section of electron density in vicinity of dimer interface and Trp-215-Ser-218 viewed down the local twofold axis. Only regions of  $\rho > 0.5 \text{ e}\text{\AA}^{-3}$  shown; position of local twofold axis indicated by cross; broken contour corresponds to twofold rotation of lower-right density; cross-hatching indicates regions lacking twofold correspondence; difference electron density between independent molecules is superimposed with bolder lines; solid, positive; dotted, negative; contours at  $0.15 \text{ e}\text{\AA}^{-3}$ , beginning with  $0.6 \text{ e}\text{\AA}^{-3}$ .

suitable heavy atom derivatives. For instance, some of the heavy atom derivatives deviated from local twofold symmetry by not showing twofold equivalent substitutions. This can be seen from Table I which summarizes the six heavy atom derivatives used for phase determination; the positions marked with asterisks for  $\delta_2$ , the positional deviation from local twofold symmetry, have no twofold counterpart in the structure.<sup>1</sup> Although some of the deviations in Table I are the result of intermolecular binding sites which do not strictly have a twofold equivalent (uranyl derivative prime occupancy sites), the majority of the deviations simply reflect differences in substitution between the two molecules. It can also be seen from Table I that when the heavy atom derivatives display local twofold symmetry, the symmetry manifests itself in a rather exact way ( $\sigma(\delta_2) \sim \pm 0.5 \text{ \AA}$ ,  $\sigma(Z) \sim \pm 3 \text{ electrons}$ ).

The interaction of the heavy atoms in different ways in the two molecules implies the molecules are different in some way in the vicinity of the substitution. This in turn implies variability in the tertiary structure. From the magnitudes and the extent of the deviations, it can be seen that the differences are generally small but significant.

#### Dimer Interface

Since the local twofold axis is situated approximately parallel to the  $a^*$  crystallographic direction, an initial position for the axis was determined by examining sections of the electron density perpendicular to  $a^*$ . The transformation between the two molecules was expressed by a rotation matrix and a translation vector. Values of the rotation matrix and translation vector were determined which minimized the square of the difference in the electron density between the two molecules. This was carried out by least-squares procedures using the electron density map at  $2.8\text{-\AA}$  resolution. The correlation coefficient (Cohen *et al.*, 1970) between the two molecules,  $c_{12}$ , was initially 0.77 and it converged to 0.82

$$c_{12} = \Sigma(\rho_1 - \bar{\rho}_1)(\rho_2 - \bar{\rho}_2) / [\Sigma(\rho_1 - \bar{\rho}_1)^2 \Sigma(\rho_2 - \bar{\rho}_2)^2]^{1/2}$$

<sup>1</sup> For the coordinates of the heavy atoms, see Tulinsky *et al.* (1973).

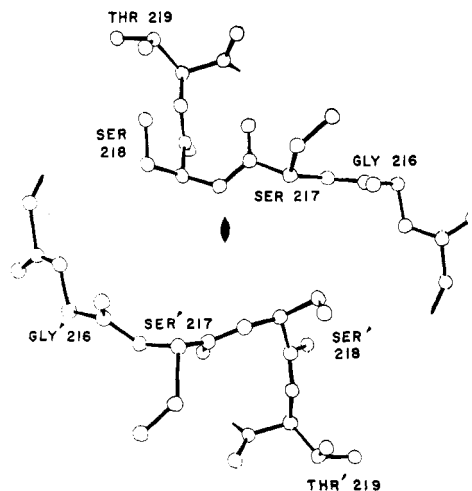


FIGURE 3: Drawing of  $\alpha$ -chymotrypsin model in vicinity of Trp-215-Ser-218 viewed down the local twofold axis. Position of twofold axis indicated by appropriate symbol.

in two cycles of refinement, where  $\bar{\rho}$  denotes the mean value of the electron density within the molecular boundaries (essentially excluding solvent regions). An examination of the difference electron density between the two molecules at this stage revealed a large number of peaks greater than  $0.7 \text{ e}\text{\AA}^{-3}$  or about three times the expected standard deviation of the difference density.<sup>2</sup> The regions of the electron density corresponding to these difference peaks (approximately 16% of the density or the equivalent of about 35–40 amino acid residues or about one-sixth of a molecule) were excluded in another cycle of least-squares refinement. The rotation matrix–translation vector remained essentially unaltered but the correlation coefficient between the two molecules increased significantly to 0.86. The final rotation matrix proved to correspond closely to a twofold symmetry operation ( $179.6 \pm 0.2^\circ$ ) and the estimated standard error in the final position of the local twofold axis was about  $\pm 0.3 \text{ \AA}$  (Tulinsky *et al.*, 1973).

Figure 2 shows a section of the electron density in the dimer interface region passing close to the main chain from Trp-215 to Ser-218 with a difference electron density superimposed (peak height of the native density  $\sim 1.0\text{--}1.2 \text{ e}\text{\AA}^{-3}$ ). From Figure 2, it can be seen that the positions of Ser-217, Ser-218, and the  $C_\alpha$  and  $C_\beta$  atoms of Trp-215 deviate up to  $2.5 \text{ \AA}$  from local twofold symmetry. The chains of the two molecules are approximately parallel to each other in this region; however, one chain approaches within  $1.75 \text{ \AA}$  of the local twofold axis while the other remains at a more distant  $4.0 \text{ \AA}$  (Figure 3). In addition, the chains are displaced by about  $2.0 \text{ \AA}$  with respect to each other along the twofold direction. From Figure 3, it can also be seen that the main chain conformations are slightly different and that the side chains of Ser-217 and Ser-218 have different orientations which lead to different hydrogen bonding possibilities. The hydrogen bonding scheme in this region is very complex since the hydroxyl groups from six side chains occur within an area of about  $6 \text{ \AA}$  in diameter

<sup>2</sup> The standard deviation of the native electron density was taken to be  $\sigma^2(\rho) = (1/V) \Sigma |F(hkl)|^2 (1 - m^2) = 0.18 \text{ e}\text{\AA}^{-3}$ , where  $V$  is the volume of the unit cell,  $m$  is the figure of merit of structure amplitude  $|F(hkl)|$ , and the summation is over all  $(hkl)$  (Blow and Crick, 1959). The standard deviation of the difference electron density is therefore  $(2)^{1/2} \times 0.18 = 0.25 \text{ e}\text{\AA}^{-3}$ . This agrees well with the root-mean-square (rms) value of the difference density in regions where the structures of the two molecules are the same (e.g., rms  $\Delta\rho < 0.5 \text{ e}\text{\AA}^{-3}$  between internal and central regions of the independent molecules).

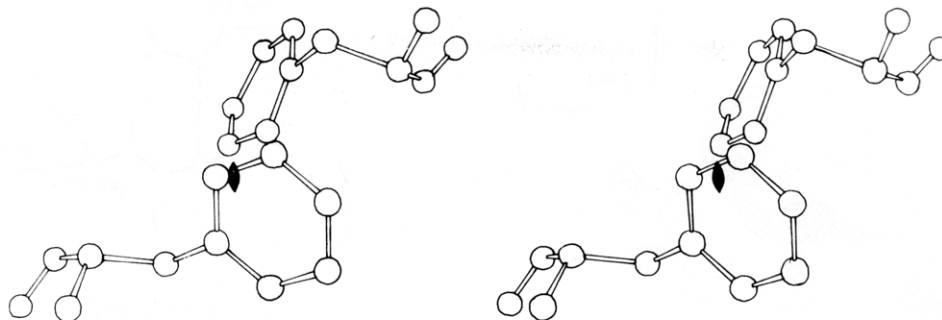


FIGURE 4: Stereoscopic diagram of Phe-39 viewed down the local twofold axis; position of twofold axis indicated by appropriate symbol.

(Ser-217, Ser-218, Thr-219, Ser-221, Ser-223, Thr-224). The situation is further complicated by the presence of at least two localized species of the mother liquor, one of which is a sulfate ion (see below) and the other probably a water molecule. Finally, since Ser-214–Gly-216 of this region have been implicated in a substrate binding interaction (Segal *et al.*, 1971), the observed differences in tertiary structure might be related to differences in competitive inhibitor binding which we observe with the independent  $\alpha$ -chymotrypsin molecules (unpublished results).

Another outstanding deviation from local twofold symmetry in the interface region occurs with Phe-39. This can be seen from Figure 4 which views the independent Phe-39 residues stereoscopically down the local twofold axis. It can be seen that the orientations of the phenyl groups differ by an approximate  $180^\circ$  rotation around the  $C_\alpha$ – $C_\beta$  bond with the centers of the resulting phenyl rings being about 4.5 Å apart.

It is interesting to note that since the position of the phenyl group of Phe-39 of both molecules is practically on the local twofold axis, neither monomeric unit can form a dimer with itself without relieving the impossible van der Waals contacts implied. The Trp-215–Ser-218 region is different in that here it is not clear whether the lack of twofold symmetry comes from repulsive or attractive interactions. In either case, the implication is that *the formation of dimer is structurally asymmetrical and dynamical in certain places of the interface region.*

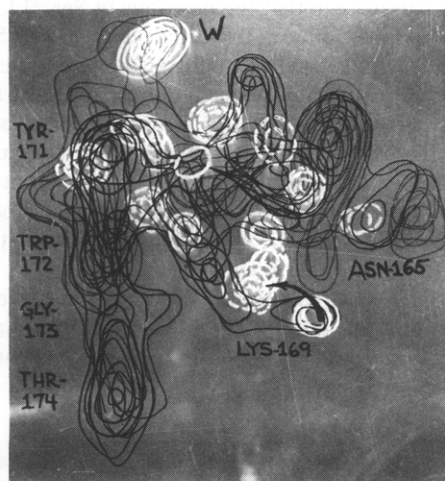


FIGURE 5: Electron density of one molecule near Met-180 loop. Density parallel to 1.5 turns of distorted helix; contours at  $0.25 \text{ e}\text{\AA}^{-3}$  ( $1.4\sigma$ ), beginning with  $0.5 \text{ e}\text{\AA}^{-3}$  ( $2.8\sigma$ ); difference electron density between the two molecules shown in white; contours at  $0.15 \text{ e}\text{\AA}^{-3}$  ( $0.5\sigma$ ), beginning with  $0.6 \text{ e}\text{\AA}^{-3}$  ( $2.5\sigma$ ); solid contour (positive) represents excess density in molecule shown; broken contour (negative) represents excess density in other molecule.

Similar observations have been made with rhombohedral zinc insulin (Blundell *et al.*, 1971a,b, 1972). Such specific observations might be the first of a more general phenomenon relating to dynamical structural adjustment common to most oligomeric structures. Although the monomeric structures are probably complementary in a geometrical way on a gross scale (see Figure 1), the details of the former appear to be finalized during the time of oligomerization.

#### Comparison of Individual Subunits

Figure 5 shows a portion of the electron density from Asn-165 through Trp-172 which represents approximately 1.5 turns of a distorted helix near the Met-180 loop. Superimposed upon the electron density in white is the difference electron density between the two molecules in this region. The gradients in the difference density are close to main chain positions and indicate that the helix is distorted differently in each molecule. In general, the difference density gradients in the map average about  $0.5$ – $0.6 \text{ e}\text{\AA}^{-4}$  and since curvatures at peak positions in the electron density are about  $0.7$ – $0.8 \text{ e}\text{\AA}^{-5}$ , the corresponding positional shifts implied are of the order of  $0.7$ – $0.8 \text{ \AA}$ ; at  $2.8$ -Å resolution, *the shifts generally correspond to groups of atoms* (e.g., partial or complete side chains, main chain amides). Figure 5 also illustrates that the side chain of Lys-169 is oriented differently in the two molecules. The difference corresponds to a  $45^\circ$  rotation of the  $\epsilon$ -amino group around the  $C_\delta$ – $C_\epsilon$  bond resulting in a linear translation of this group of about  $1.5 \text{ \AA}$  in the direction of the amide side chain of Asn-165. The peak marked W has been interpreted to be a water molecule ( $\text{SO}_4^{2-}$  has been eliminated from consideration; see next section). The water is hydrogen bonding with the hydroxyl group of Tyr-171 and appears in one enzyme molecule (electron density shown) but not the other of the asymmetric unit. Such features occur frequently but not always as prominently as seen here. Similar behavior pervades throughout most of the electron density near the surface of the molecule. On the other hand, there are regions where the two molecules are practically identical as in the main chain portion Trp-172–Gly-173–Thr-174 shown in Figure 5. Such behavior becomes prevalent toward the interior of the molecule. In these interior regions, averaging of the electron density is certainly a useful procedure.

The comparison of the two molecules can be summarized in general terms by saying that the more extensive and prominent differences reside in a  $5$ – $6$ -Å shell of density around the surface of the molecule (one–two peptide layers) and that the number of differences falls off sharply toward the interior. The differences are most often associated with the side chains and less with the main chains. The conformations of the main chains of the two molecules are practically the same toward the

TABLE II: Nonpolar Cavity,  $\alpha$ -Chymotrypsin.<sup>a</sup>

Level	$\alpha$ -CHT	BT	DFT	Th	BCA	BCB	PE
1	Trp-237	Trp		Trp	Trp	Trp	Trp
	Thr-241	Thr	Thr	Val	Thr	Thr	Val
2	Trp-51	Trp		Trp	Trp	Trp	Trp
	Ile-103	Ile	Ile	Ile	Ile	Ile	Ile
	Leu-105	Leu	Leu	Leu	Leu	Leu	Leu
	Leu-234	Tyr		Lys	Leu	Leu	Tyr
	Val-235	Val		Leu	Val	Met	Ile
	Val-238	Ile	Ile	Ile	Val	Val	Ile
	Leu-242	Ile	Ile	Ile	Leu	Leu	Ile
3	Ile-47	Ile	Ile	Ile	Ile	Ile	Ile
	Val-53	Val			Val	Val	Met
	Leu-123	Leu	Leu		Leu	Leu	Leu
	Pro-124	Pro	Pro		Pro	Pro	Pro
	Ile-212	Ile	Ile	Ile	Ile	Ile	Val
	Val-231	Val		Val	Val	Val	Val
	Trp-29	Tyr		Trp	Trp	Trp	Ser
4	Val-121	Ile	Ile		Val	Val	Gly
	Val-200	Val	Val	Val	Val	Val	His
	Leu-209	Leu		Gln	Leu	Leu	Val

<sup>a</sup> Abbreviations used are: CHT, chymotrypsin; BT, bovine trypsin; DFT, dogfish trypsin; Th, thrombin; BCA, bovine chymotrypsin A; BCB, bovine chymotrypsin B; PE, pig elastase.

interior. Near the surface, the most frequent differences occur with Lys, Gln, and Asn side chains, where, more often than not, they appear to show different orientations and configurations in the two molecules (the electron density of Lys occasionally shows two orientations within the same molecule; e.g., Lys-177). On the other hand, Glu and Asp side chains display surprisingly close twofold correspondence in the two molecules. The smallest number of differences on the molecular surface accompanies Ser and Thr, but being fairly small in size this might be due to their generally lower electron density so that differences approach background fluctuations.

The differences appearing in the interior of the molecule are usually associated with Leu and Ile side chains and, as on the surface, less frequently with the main chain of the protein. Pro and Cys nearly always show some differences, which simply suggest better order in one molecule or the other because the differences are probably due to the generally higher electron density of these residues (approaching  $2.0 \text{ e}\text{\AA}^{-3}$ ).

A region of the electron density which shows essentially no differences between the two molecules is one conspicuously associated with a nonpolar cavity (about 8–9 Å in diameter) just off the surface of the molecule near the  $\alpha$ -helical region at the Asn-245 carboxyl terminus. Most of the residues of this cavity are also in the contact region between the surfaces of cylinders 1 and 2 of the MRC structure (Birktoft and Blow, 1972). The relative arrangement of the 18 or so residues of the shell comprising this cavity is shown in a schematic way in Figure 6 where increasingly higher level indicates deeper penetration into the molecule. Besides the two residues of level 1, Leu-123, Leu-234, and Val-235 have reasonable access to the surface. Table II lists a comparison of residues in these positions after optimal sequential alignment of a number of serine proteases thought to be evolutionarily related (Hartley, 1970; Stroud *et al.*, 1971). As noted elsewhere, it can be seen that the chemical similarity and the invariance of the residues

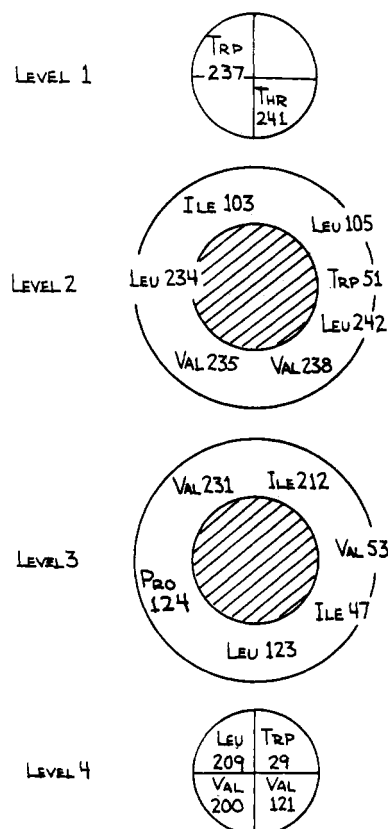


FIGURE 6: Schematic of nonpolar cavity. Increasing level number corresponds to deeper inner penetration of the molecule; cross-hatching corresponds to vacant space of the cavity (8–9 Å in diameter).

in this region are truly remarkable (Shotton and Hartley, 1970) and that they are probably related to the observed structural invariance between the two molecules. Position 234 shows the most homologous variability; however, the side chain of this position has access to the surface. Thus, if the polar end of Lys (in Th) and Tyr (in bovine trypsin and pig elastase) extends toward the surface, the nonpolarity of the cavity remains essentially unimpaired by the substitution. Finally, it is of interest to note that pig elastase is not homologous in level 4 of the nonpolar shell.

#### Localized Sulfate Ions

Since the crystals used in our studies are stored in ~75% saturated  $(\text{NH}_4)_2\text{SO}_4$  at about pH 4.2, the mother liquor of the crystals consists primarily of water and ions derivable from  $(\text{NH}_4)_2\text{SO}_4$ . At an early stage in the interpretation of the 2.8-Å resolution electron density map, it was suspected that not all the peaks unassigned to the protein represent localized water molecules, although a great majority probably do. This led to investigating the effect of changing the nature of the soaking solution of crystals by replacing  $(\text{NH}_4)_2\text{SO}_4$  with  $(\text{NH}_4)_2\text{SeO}_4$  (Tulinsky and Wright, 1973). No apparent complications were introduced by the procedure since the solubilities of the two salts are similar and the dissociation constants of the respective acids are about the same. The results of this simple experiment proved to be most informative: (1)  $\text{SO}_4^{2-}$  ions are localized in the structure and participate in solvating the enzyme; (2) the  $\text{SO}_4^{2-}$  ions exchange with  $\text{SeO}_4^{2-}$ ; (3) the  $\text{SO}_4^{2-}$  ions solvate with a range of binding constants; and (4) two  $\text{SO}_4^{2-}$  ions participate in a hydrogen-

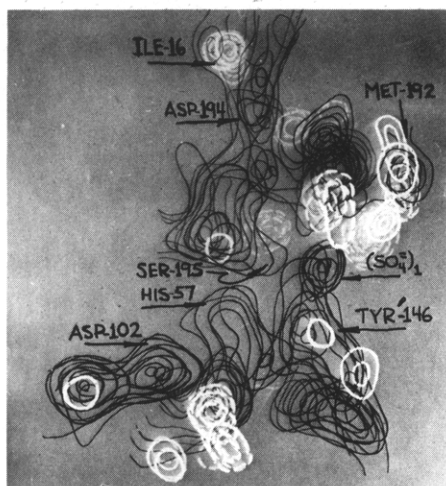


FIGURE 7: Electron density of the active-site region of one molecule. Difference electron density between two molecules shown in white; contours and their meaning as in Figure 5; electron density corresponding to various side chains indicated by arrows; density of main chain immediately adjacent.

bonding scheme which appears to be an important interaction in stabilizing the dimeric structure. The latter ions form bridges, in a reciprocating manner between the independent molecules, which involve the catalytically crucial Ser-195 of one molecule and the phenolic hydroxyl group of terminal Tyr-146 of the other molecule.

We originally uncovered the range of binding constants of the  $\text{SO}_4^{2-}$  ions inadvertently. The diffraction pattern of crystals which only had a  $\text{SeO}_4^{2-}:\text{SO}_4^{2-}$  ratio of 5:1 was examined and since there were prominent changes in intensities, three-dimensional intensity data to 2.8-Å resolution were measured and a difference electron density map was computed. The difference map revealed two dominant peaks ( $\sim 0.5 \text{ e}\text{\AA}^{-3}$ ) which superimposed upon two peaks ( $0.86$  and  $0.85 \text{ e}\text{\AA}^{-3}$ ) of the electron density of the protein. The latter were already suspected to be due to the mother liquor of the crystals. Thus, these peaks have been interpreted to be  $\text{SO}_4^{2-}$  ions, and they are also the ones that bridge between the two independent molecules. Furthermore, each ion is located about 4.5 Å from the imidazole of His-57. Since the imidazole side chain of His-57 at pH 4.2 is an imidazolium ion, the positive charge of the latter and the charge of the  $\text{SO}_4^{2-}$  must neutralize each other to some extent. Moreover, the sulfate ions are accompanied by a peak in the electron density ( $0.75 \text{ e}\text{\AA}^{-3}$ ) about 4.0 Å away which has tentatively been assigned to that of a cation, thereby neutralizing more of the charge of the sulfate ion, which is consistent with the  $\text{SO}_4^{2-}$  ions being located internally between monomers in the dimer structure. Increasing the  $\text{SeO}_4^{2-}:\text{SO}_4^{2-}$  ratio to about 20:1 did not cause any appreciable changes to the intensity distribution observed with 5:1 crystals; however, increasing the ratio to 100:1 produced a host of additional changes which corresponded to additional exchange of  $\text{SO}_4^{2-}$  ions. From the foregoing discussion, it can be inferred that the bridging  $\text{SO}_4^{2-}$  ions, observed initially in the 5:1 experiment, are extremely facile toward exchange. The facile nature of the bridging  $\text{SO}_4^{2-}$  ions also manifests itself when they are displaced from the active-site region by irreversible and competitive inhibitors and substrate-like molecules (unpublished results).

Table III summarizes the results of the ( $\text{SO}_4^{2-}-\text{SeO}_4^{2-}$ ) exchange experiments and also includes the results obtained with crystals of  $\alpha$ -chymotrypsin grown from  $(\text{NH}_4)_2\text{SeO}_4$

TABLE III: Summary of ( $\text{SO}_4^{2-}-\text{SeO}_4^{2-}$ ) Experiments.<sup>a</sup>

	$\Delta\rho$ $\text{SO}_4^{2-}$ (5:1)	$\Delta\rho$ (100:1)	$\Delta\rho$ ( $\text{SeO}_4^{2-}$ )	$\rho_{\text{CHT}}$	Environment
{1 1'}	0.50 0.57	0.57 0.55	0.76 0.64	0.86 0.85	Gly-193, Ser-195, Tyr'-146 (carboxyl terminus, B chain)
{2 2'}		0.28	0.24	0.96 0.71	Asn-95, Lys-177
{3 3'}		0.27 0.24	0.27 0.13	1.17 0.88	Ser-217, Thr-224
{4 4'}		0.17 0.23	0.14 0.18	0.82 0.82	Asp-153, Arg-154
{5 5'}		0.23 0.16	0.18 0.13	0.71 0.73	Thr-61, Ala'-149 (amino terminus, C chain)
{6 6'}		0.17 0.21	<0.10 0.11	0.93 0.69	Cys-1 (amino terminus, A chain), Val-3
{7 7'}		0.18 0.13	0.20 0.15	0.84 0.66	Asn-236

<sup>a</sup>  $\Delta\rho$ , peak heights given in  $\text{e}\text{\AA}^{-3}$  from difference map using  $(|F|_{\text{P+Se}} - |F|_{\text{P}}) \exp(i\alpha_{\text{P}})$  as coefficients;  $\rho_{\text{CHT}}$ , corresponding peak heights in native enzyme electron density (*i.e.*,  $\text{SO}_4^{2-}$ ); prime notation denotes local twofold equivalent.

(column designated by  $\text{SeO}_4^{2-}$ ). The latter experiment was performed in order to investigate the possibility of non-exchangeable  $\text{SO}_4^{2-}$  ions. From Table III, it can be seen that: (1) all of the  $\text{SO}_4^{2-}$  ions are exchangeable; (2) the electron density regions in  $\alpha$ -chymotrypsin corresponding to  $\text{SO}_4^{2-}$  ions are generally exceptionally large; and (3) the  $\text{SO}_4^{2-}$  ions appear in reasonable proximities for interaction with the enzyme (*e.g.*, ion pair and/or hydrogen bonding). In addition, ( $\text{SO}_4^{2-}$ )-2 does not show a twofold equivalence in any of the experiments. The positions of ( $\text{SO}_4^{2-}$ )-5 and -5' deviate from twofold symmetry by about 3.0 Å and the other  $\text{SO}_4^{2-}$  ion pairs behave similarly. Since the heavy atom derivatives indicated that twofold correspondence can be as precise as  $\sim 0.5$  Å, the  $\text{SO}_4^{2-}$  ions show significant departures from the symmetry. The larger average deviation of the  $\text{SO}_4^{2-}$  ions from twofold symmetry is probably related to their generally weaker interaction with the enzyme as compared to the heavy atom derivatives.

#### Active-Site Region

Figure 7 shows a portion of the 2.8 Å resolution electron density map in the region of the active site of one molecule viewed approximately parallel to the local twofold axis; as before, superimposed upon the electron density is the difference electron density between the two molecules in the asymmetric unit. From Figure 7, it can be seen that although the two active sites are generally similar, there are a number of significant differences between the two molecules. The largest difference in this region occurs with Met-192. If the sulfur atoms of the two Met residues showed exact twofold symmetry, the distance between the sulfur atoms would be  $< 3.0$  Å. To relieve this potential crowding, one Met side chain is translated with respect to the other by about 1.5 Å



along the direction of the local twofold axis. Other differences in Figure 7 are associated with: (1) the position of the bridging  $\text{SO}_4^{2-}$  ions between the two molecules (see above); (2) the main chain portion of His-57; and (3) the positions of the side chains of the B-chain amino terminus (Ile-16) and the carboxylate group of Asp-194.

#### Derivatives of $\alpha$ -Chymotrypsin

During the course of our work, we have obtained three-dimensional 2.8-Å resolution structures for about 30 derivatives of  $\alpha$ -chymotrypsin (excluding heavy atom derivatives). These derivatives generally fall into classes, each class usually being of more interest than the specific members which comprise it. The classes can be conveniently grouped as: (1) irreversible inhibitors, (2) competitive reversible inhibitors, (3) substrate analogs, (4) structural changes with change of pH, (5) ( $\text{SO}_4^{2-}$ - $\text{SeO}_4^{2-}$ ) exchange, (6) transition-state analogs, and (7) Met-192 alkylation. The results of these studies ranged from fairly spectacular substitutions with tosyl and pipsyl ( $\sim 1.0 \text{ e}\text{\AA}^{-3}$ ) and phenylethaneboronic acid ( $\sim 0.45 \text{ e}\text{\AA}^{-3}$ ) to disappointingly small changes with *N*-L-fPhe ( $\sim 0.26 \text{ e}\text{\AA}^{-3}$ ) and *N*-L-fTrp, the latter additionally being studied at pH values of 4.2 and 6.7 ( $\sim 0.20 \text{ e}\text{\AA}^{-3}$ ). Furthermore, the twofold behavior of the derivative changes was generally variable and unpredictable. At times, the twofold symmetry of the substitution was exceptionally well preserved (e.g., tosylation), while at others, large and significant departures occurred from the local symmetry (e.g., *N*-pipsyl-L-phenylalanyl chloromethyl ketone, toluenesulfonylamide). In most of the derivatives, changes in the native structure accompanying the substitution generally lacked twofold correspondence. With the chloromethyl ketone reagent, the two active sites showed different occupancies of substitution (ratio of about 3:2) and, in addition, an auxiliary binding site was operative in one molecule but not the other of the dimer (Tulinsky *et al.*, 1971). This site is some 20 Å from the active site and is formed by a cluster of three Trp residues (27, 29, and 207), Pro-28, and Pro-8. The latter residue is located near the carboxyl terminus of the A chain. The site is apparently inoperative in one of the molecules because Pro-8 and its immediate residues make a closer contact to the Trp cluster, an intramolecular contact which is also fairly intimate in the other molecule, and thus excludes accessibility to the cluster by the aromatic moiety. Similar spatial clustering of other aromatic residues was observed at different places in the molecule (His-40, Phe-41, Trp-141; Trp-51, Phe-89, Trp-237; Tyr-171, Trp-172, Trp-215) and it has also been reported in human carbonic anhydrase C (Liljas *et al.*, 1972). The spectacular manner in which the aromatic residues tend to aggregate within the molecular structure of  $\alpha$ -chymotrypsin suggests that the phenomenon might be of fundamental importance in imparting some stability to the tertiary structure through the interaction of the delocalized electrons of the aromatic side chains.

The derivatives involving a change in structure with a change in pH of enzyme crystals also proved to be informative with respect to variability in the tertiary structure (Vandlen and Tulinsky, 1971b, 1973). When the pH of crystals is raised from 4.2, a structural rearrangement occurs over a fairly sharply defined pH range (0.2–0.3 pH unit) around pH 5.4. Thereafter, up to pH  $\sim 7.0$ , the structure remains essentially constant as evidenced by the diffraction pattern throughout this pH range. The difference electron density map at 2.8-Å resolution between crystals of native enzyme at pH 6.7 and

4.2 showed a large number of significant changes in structure, the greatest majority of them occurring near the dimer interface region. The largest changes in the electron density ( $0.35 \text{ e}\text{\AA}^{-3}$ ) were associated with His-40 (both molecules) and a segment of chain near the carboxyl terminus of the B chain (Thr-139–Tyr-146). The latter changes appear to be involved with the association–dissociation of the dimer and the B-chain terminus changes show fairly good twofold symmetry. The change associated with His-40 undoubtedly involves loss of a proton and is accompanied by a rotation of the imidazole ring in its plane toward the carbonyl of Gly-193. This change does not show good twofold symmetry. Another region important to dimer stability involves an ion pair interaction (Asp-64, Ala-149) and this region also shows changes in structure with pH. Finally, the active-site regions of the two molecules both undergo small conformational changes with change in pH. The set of changes of one molecule tends to make it resemble the other molecule more closely; however, nontwofold changes effectively prevent the two active-site regions from achieving a twofold correspondence (Vandlen and Tulinsky, 1973).

#### Comparison with the MRC Structure

We have carried out some comparisons between our work and results reported by the MRC group (Birktoft and Blow, 1972). However, for a number of reasons, the comparisons are only of a preliminary nature. For one thing, our refinement of the structure is not yet completed; for another, we had to compare our native structure with that of the MRC tosyl- $\alpha$ -chymotrypsin structure. Moreover, the comparison involved the structure of one molecule of the dimer and the structure derived from averaging the tosyl- $\alpha$ -chymotrypsin electron densities of the two crystallographically independent molecules in the asymmetric unit.

The original MRC Kendrew model coordinates were initially adjusted (Birktoft and Blow, 1972) to correspond to the structural geometries of known amino acids using Diamond's model building program (Diamond, 1966); the same was done with our model coordinates. The MRC adjusted model coordinates were then refined by the real space refinement procedure (Diamond, 1971) which optimizes the fit of a calculated electron density of the protein model to the observed electron density distribution; one cycle of such a refinement was also performed on our adjusted model coordinates. Finally, the refined MRC coordinates were additionally given one cycle of energy refinement (Levitt and Lifson, 1969).

The comparison of the two structures can be summarized briefly as follows. The main chain coordinates of the MRC average structure agree fairly well with those of one molecule of the dimer indicating again that the main chain conformations of the independent molecules are essentially the same (root-mean-square (rms)  $\Delta \sim 1.3 \text{ Å}$ , all C, O, N,  $\text{C}_\alpha$ ). The best agreement occurs with the C-chain terminus  $\alpha$  helix (rms  $\Delta \sim 0.8 \text{ Å}$ ) and this also corresponds approximately to the rms  $\Delta$  between the two independent molecules in regions of no structural differences in the present work. The regions showing variability in tertiary structure in our work possess significant discrepancies in the above comparison: Glu-70–Ser-77 (rms  $\Delta \sim 3.5 \text{ Å}$ , similarly observed by the MRC); Gly-216–Thr-219 ( $\sim 2.6 \text{ Å}$ ); Thr-174–Ile-176 ( $\sim 2.3 \text{ Å}$ ); Tyr-146, Ala-149, at chain termini and still other places. Furthermore, a characteristic of the main chain differences between the MRC structure and ours is that they are generally confined to small regions (di- or tripeptide units). The agree-

ment between the side-chain orientations and their stereochemistry is considerably worse (rms  $\Delta \sim 2.3$  Å). These larger differences are due to: (1) variability in the tertiary structure, (2) differing interpretations of the electron density by the two groups, and (3) the manner in which some of the MRC side-chain structure was fixed.<sup>3</sup> On the other hand, some of the larger side chains such as Trp, Pro, Phe, and Tyr frequently show excellent agreement (rms  $\Delta < 1.0$  Å).

### Concluding Remarks

The lack of precise twofold symmetry between the two molecules in the asymmetric unit of  $\alpha$ -chymotrypsin can arise from several different causes. It can result from the different environments of the two molecules of the crystallographic asymmetric unit which lead to different intermolecular contacts. This would include, to some extent, the nature of localized solvent molecules and ions and the surrounding solution. The net effect of the different environments would be to exert different distorting intermolecular interactions on the two molecules. However, since the number of close intermolecular contacts is relatively small, such distortions can account for only part of the observed differences. Alternatively, the lack of symmetry might be inherent in the dimeric structure. This is certainly obvious in the dimer interface region where integration of the molecules involves a number of close contacts which are achieved by the molecules reorganizing to accommodate each other. In the process an arrangement results in which the two molecules no longer have precisely the same structure. Conversely, the dissociation to monomers must also be structurally dynamical with the molecules rearranging to achieve maximum stability in the monomeric state. Similar changes, but more distant from the interface, might also be the result of dimerization, but for less obvious reasons. Finally, some of the observed side-chain surface variability might even be of a more general nature indicating the extent of adaptability of the tertiary structure and conceivably could be present in functioning molecules in solution and in biological systems.<sup>4</sup> From the extent of the observed side-chain variability on the surface, it would seem that the large amount of the localized surface structure commonly observed in X-ray crystallographic determinations of proteins might be due in part to the influence of the crystal structure and that true surface localization probably occurs at a lesser level. This, of course, would not apply to such specialized regions as active sites or regions where intramolecular hydrogen bonding or other stabilizing interactions can occur. These regions might even include Asp and Glu residues since they showed a

high degree of localization in the independent monomer molecules of  $\alpha$ -chymotrypsin.

### References

- Aune, K. C. and Timasheff, S. N. (1971), *Biochemistry* 10, 1609.
- Birktoft, J. J., and Blow, D. M. (1972), *J. Mol. Biol.* 68, 187.
- Birktoft, J. J., Matthews, B. W., and Blow, D. M. (1969), *Biochem. Biophys. Res. Commun.* 36, 131.
- Blow, D. M., and Crick, F. H. C. (1959), *Acta Crystallogr.* 12, 794.
- Blow, D. M., Rossmann, M. G., and Jeffery, R. A. (1964), *J. Mol. Biol.* 8, 65.
- Blundell, T. L., Cutfield, J. F., Cutfield, S. M., Dodson, E. M., Dodson, G. G., Hodgkin, D. C., Mercola, D. A., and Vijayan, M. (1971a), *Nature (London)* 231, 506.
- Blundell, T. L., Cutfield, J. F., Dodson, G. G., Hodgkin, D. C., and Mercola, D. A. (1971b), *Cold Spring Harbor Symp. Quant. Biol.* 36, 233.
- Blundell, T. L., Dodson, G. G., Hodgkin, D. C., and Mercola, D. A. (1972), *Advan. Protein Chem.* 26, 279.
- Cohen, G. H., Matthews, B. W., and Davies, D. R. (1970), *Acta Crystallogr. Sect. B* 26, 1062.
- Diamond, R. (1966), *Acta Crystallogr.* 21, 253.
- Diamond, R. (1971), *Acta Crystallogr., Sect. A*, 27, 436.
- Egan, R., Michel, H. O., Schlueter, R., and Jandorf, B. J. (1957), *Arch. Biochem. Biophys.* 66, 366.
- Hartley, B. S. (1970), *Phil. Trans. Roy. Soc. London, Ser. B* 257, 77.
- Levitt, M., and Lifson, S. (1969), *J. Mol. Biol.* 46, 269.
- Liljas, A., Kannan, K. K., Bergsten, P. C., Waara, I., Fridborg, K., Strandberg, B., Carlsson, U., Jarup, L., Lovgren, S., and Petef, M. (1972), *Nature (London)*, 235, 131.
- Segal, D. M., Powers, J. C., Cohen, G. H., Davies, D. R., and Wilcox, P. E. (1971), *Biochemistry* 10, 3728.
- Shotton, D. M., and Hartley, B. S. (1970), *Nature (London)* 225, 802.
- Sigler, P. B., Blow, D. M., Matthews, B. W., and Henderson, R. (1968), *J. Mol. Biol.* 35, 143.
- Sigler, P. B., Jeffery, B. A., Matthews, R. B., and Blow, D. M. (1966), *J. Mol. Biol.* 15, 175.
- Steiner, R. F. (1954), *Arch. Biochem. Biophys.* 53, 457.
- Steitz, T. A., Henderson, R., and Blow, D. M. (1969), *J. Mol. Biol.* 46, 337.
- Stroud, R. M., Kay, L. M., and Dickerson, R. E. (1971), *Cold Spring Harbor Symp. Quant. Biol.* 36, 125.
- Tulinsky, A., Coddington, P. W., and Vandlen, R. L. (1971), Abstracts, Winter Meeting of the American Crystallographic Association, Columbia, S. C., Feb. No. K3.
- Tulinsky, A., Mani, N. V., Morimoto, C. N., and Vandlen, R. L. (1973), *Acta Crystallogr. Sect. B* 29, 1309.
- Tulinsky, A., and Wright, L. H. (1973), *J. Mol. Biol.* (in press).
- Vandlen, R. L., and Tulinsky, A. (1971a), *Acta Crystallogr., Sect. B* 27, 437.
- Vandlen, R. L., and Tulinsky, A. (1971b), Abstracts, 67th Annual Meeting of the American Society of Biological Chemists, San Francisco, Calif., June, No. 444.
- Vandlen, R. L., and Tulinsky, A. (1973), *Biochemistry* 12, 4193.

<sup>3</sup> When the MRC average map was ambiguous, the electron densities of the individual molecules were consulted and the clearer alternative was chosen for the model. Thus, the final structure is composed of side chains derived from the average electron density and the electron densities of the individual molecules. If there were no variability in side-chain structure, such an interchange would be acceptable; however, this is precisely where we observe the most variability in tertiary structure and the area of largest number of discrepancies between our work and that of the MRC.

<sup>4</sup> The foregoing does not intend to imply randomness in side-chain orientation and configuration on the surface but suggests, rather, that a number of energetically comparable orientations and configurations might be possible.